EJECTION AND IMPACT ANGLES OF SALTATING PARTICLES MEASURED WITH A HIGH-SPEED CAMERA

M. Raddatz, H.-J. Schönfeldt

ABSTRACT

3D and 2D trajectory data of sand grains saltating over a bed are presented from high-speed camera measurements. They were obtained at Zingst peninsula and in laboratory using a wind tunnel. Trajectories, calculated with a Runge-Kutta procedure, using values of the mean wind profile and the air flow were fitted to the measured ones. The trajectory with the lowest RMSE against the measured one was used to estimate the grain diameter of the saltating grain. Also ejection and impact angle, ejection and impact speed of the grain were determined. The results confirm earlier findings that ejection angles decreases with increasing grain diameter. Ejection angles between 57° and 27° for fine (63-200 µm) and middle (200-630 µm) ejecta and between 38° and 20° for coarse grains (630-2000 µm) were found. The impact angle β increases with increasing grain diameter. Impact angles between 8° and 15° for fine impactors and between 12° and 36° for middle and coarse grains were found. Additionally the ratio between the mean ejection angle α and mean impact angle β, which decrease with increasing grain diameter (Rice et al., 1995), could be confirmed. The ration between the ejection speed u_e and impact speed u_i was found nearly the same for all determined grain sizes, but the grains ejected from the bed had an average speed of one order of magnitude less than the impact speed.

1. INTRODUCTION

Desertification is a major problem connected with the global climate. Grassland worldwide desolates into dry land or even deserts because of overgrazing, wrong fertilization and irrigation. Also commercial logging is a problem because the lost shading of the trees will increase evaporation of the soil. The structure of the soil gets porous. At this stage it is easy for wind and rain to blow off and wash out surface particles. Understanding the appearance of desertification it is crucial to conceive the basic mechanisms of sand transport. Dust emission generated by wind erosion is by far the largest source of aerosols which directly or indirectly influence the atmospheric radiation balance and hence global climatic variations (Shao, 2000). The Taklimakan desert in central Asia is extending faster than any other desert in the world. Hyper arid climate conditions and strong winds in the eastern part of the desert accelerate the rambling of the dunes (Laity, 2008). According to the UNCCD (*United Nations Convention to Combat Desertification*) office there are 110 countries and over one billion people threatened by desertification worldwide.

2. EXPERIMENTAL SETUP AND METHOD

Measurements of moving particles over a surface were done by several researchers like Willetts and Rice (1995), Anderson and Haff (1988, 1991), McEwan and Willetts (1993) and Rioual et al. (2000). They also used high-speed cameras but they only recorded trajectories from the grains in two dimensions. For our measurements a stand with a special mirror, a swiveling holder with 20 white LED´s and a clamp for the high-speed camera were constructed. This setup allows to measure trajectories in three dimensions. Figure 1 shows the setup which was used in the measurements at the beach on Zingst peninsula. During the measurements the plate and the battery were moved a little bit side wards so that they do not disturb the air flow. The purpose of the experiments was to measure trajectories from moving grains, preferential saltating, creeping and reptating grains under natural conditions. Therefore the test area was not "cleaned". On the windward side of the measurement array there were smaller and bigger shells, some seaweed, and footsteps from tourists and sometimes sand ripples which can trigger saltation. Before starting recording high-speed movies the camera (SANYO Xacti 1010) had to be set up. The time of the video sequence was set to 10 seconds with 300 frames per second. In this mode the resolution of the video lasts 448×336 pixel. The focal point was set to 10 cm because of the dimensions of the stand. Aperture and ISO value were adjusted automatically. The zoom was changed to +1.5 to get an adequate acuity of the saltating grains. With all these adjustments a square with 1×1 mm equals a square with 7×7 pixel. Knowing this the computer program was able to convert every pixel value into a metric value. A chart including our measurement configuration was made with a CAD (*Computer Aided Design*) program. The imaginary rays from the camera and the rays from a virtual camera behind the mirror to the selected grain are shown in Figure 2. The marked bead (red dot) and the imaginary rays (black lines) are labeled with the expressions used in the program for calculating the position of the grain. Availing the virtual camera it was easier to form the three equations (Eq. 1-3) for calculating the position of the grain.

Figure 1: *Setup used at the beach in Zingst, including a plate to shield the horizon, the stand with the mirror, the swiveling holder with the LED´s and the high-speed camera. A plastic body for smoothing the air flow is fitted in front of the stand.*

$$z = \frac{x_b \cdot y_s \cdot z_{cam}}{(x_s \cdot z_{cam} + x_b \cdot y_s)} \qquad x = \frac{x_s \cdot z}{y_s} \qquad y = \frac{y_b \cdot x}{x_b}$$

Eq. 1-3

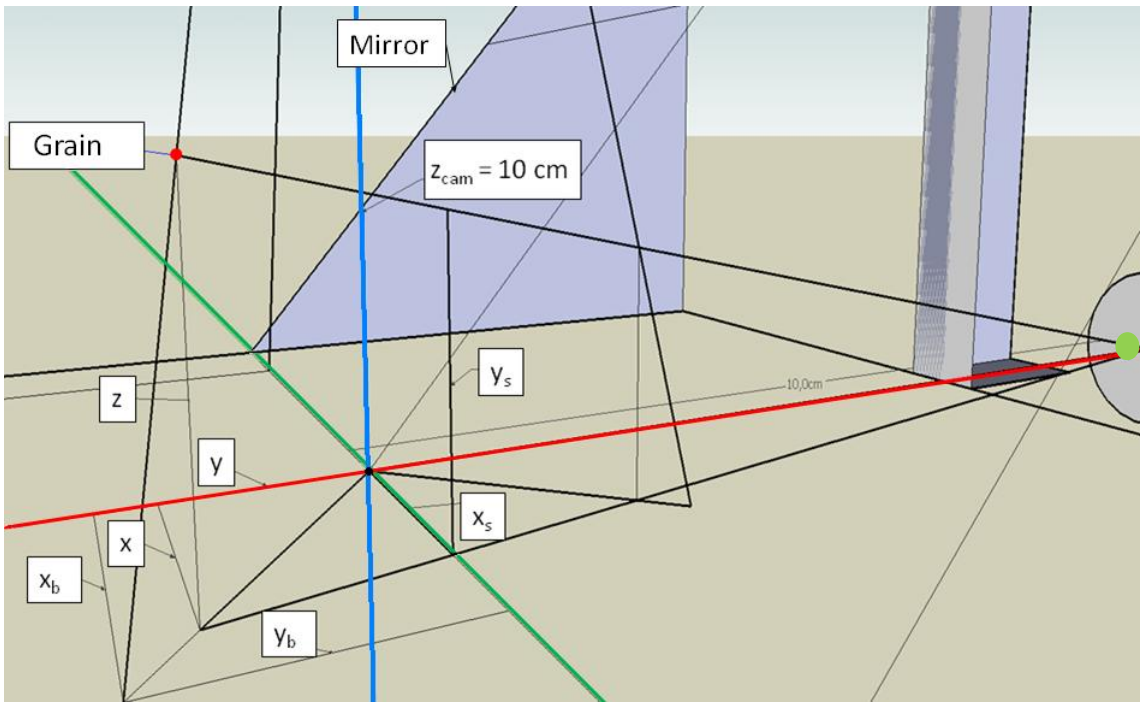

Figure 2: *CAD chart with the marked grain (red dot) and the imaginary rays (black lines) from the camera to the grain and from a virtual camera (green dot) behind the mirror to the grain. The green line symbolizes the x-axis, the red line the y-axis and the blue line the z-axis. The labeled expressions were used in the program for calculating the position of the grain.*

The whole geometry of the measurement array is very complex. Figure 3 illustrates a blueprint of the light path for better demonstration of the coherence between the grain (red dot), the camera, the mirror (blue triangle) and the virtual camera (green dot). In the upper part of the picture there is an upright projection of the configuration and in the lower part there is shown the plan view. As seen in Figure 1 a plate had to be build, to shield the horizon and to create a good contrast between the bright saltating grains and the background.

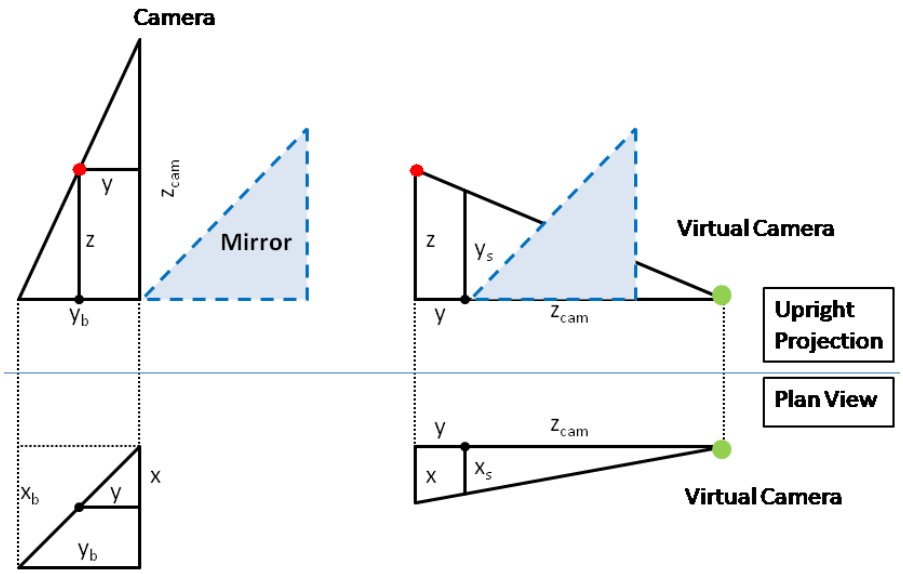

Figure 3: *Blueprint of the light path for better demonstration of the coherence between the grain (red dot), the camera and the mirror (blue triangle. It also shows the importance of the virtual camera (green dot) for forming the equations 1-3.*

Figure 4 shows a typical collision and resulting trajectory of a saltating grain. This chart also explains what is meant by a trajectory. The grain ejected by collision leaves the surface with a speed, u_e and an ejection angle α and approaches the bed with a speed, u_i and an impact angle β. Because of the non smooth trajectories of the recorded grains a Runge-Kutta procedure was included in the evaluation program. Adjusting measured values of the trajectory which are defective and scattered around the correct value the Runge-Kutta procedure calculates theoretical trajectories for 41 before given grain diameters and selects the one with the lowest RMSE (*Root Mean Square Error*) comparing to the measured trajectory. The trajectory with the lowest RMSE was then printed against the measured trajectory and symbolizes now the smooth path of the real saltating grain, see Figure 5. This procedure was done to all measured trajectories from the campaign as well as to the trajectories measured in the laboratory. Additionally, the output of the RMSE for each calculated trajectory with changed grain diameter allows an inference on the grain size of the saltating grain.

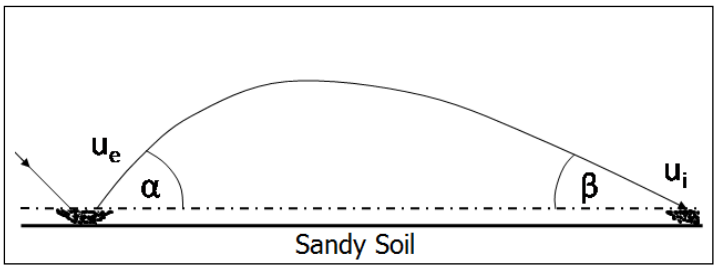

Figure 4: *Typical trajectory of saltating grains. The grain ejected by collision leaves the bed with a speed, u_e, and an angle α and approaches the bed with a speed, u_i, and an angel β.*

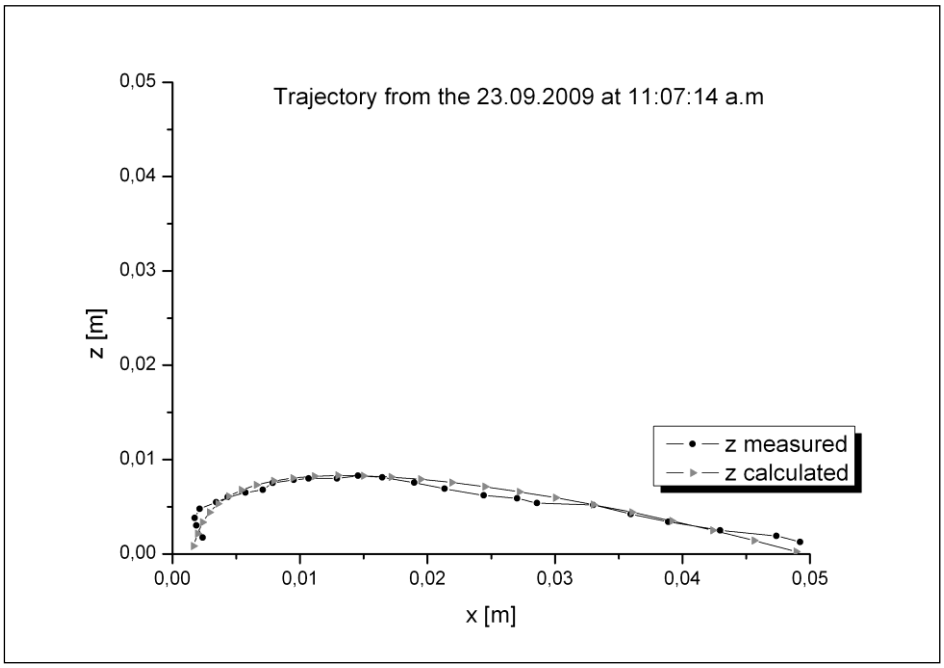

Figure 5: *Measured trajectory (dots) and the numerically approximated trajectory (triangle) with the lowest RMSE compared to the measured one.*

3. MEASUREMENTS AND DATA INTERPRETATION

First test measurements were done in the laboratory to evaluate the capabilities of the 3D trajectory analysis. Therefore a wind tunnel with a diameter of 0.5 m was used. A thin layer of sand, from the beach of Zingst peninsula, was put on a table after we installed the stand with the camera.

In September 2009 there was a campaign in Zingst at the Baltic Sea. The aim of the campaign was to record as much data as possible at the beach under natural conditions. More than 300 videos were recorded in these two weeks. Additional to the video measurements of the saltating grains a wind mast with three cup anemometers, in heights of 0.2, 1.0 and 2.0 m, was build to reconstruct the wind profile. Also an ultrasonic anemometer (*USA*) was arranged at the surface to recognize the wind direction, wind speed and also for comparing the values with the cup anemometers. Problematic were the fast changing cloudiness from clear sky to total clouded. These different illumination conditions are seen in Figure 6, and had effects on the visibility of the grains in the mirror and also over the surface.

Therefore a classification was made: 1. shady surface / mirror irradiated by the sun; 2. cloudy surface and mirror and 3. sunny surface / mirror irradiated by the sun.

Figure 6: *Different illumination conditions at the beach of Zingst. (1) shady surface / mirror irradiated by the sun; (2) cloudy surface and mirror; (3) sunny surface / mirror irradiated by the sun.*

The best and rich in contrast movies were recorded when the sun was at the zenith and the whole surface was well illuminated (3) and therefore all edges got very sharp even the grains. Also good movies were logged when the sky was totally clouded and the surface got shady (2).

4. RESULTS

For evaluation 100 representative trajectories were selected. Ejection angles typically decrease with increasing grain diameter. The results show ejection angles between 57° and 27° for fine (63-200 µm) and middle (200-630 µm) ejecta and between 38° and 20° for coarse grains (630-2000 µm). The impact angle β increases with increasing grain diameter. Impact angles between 8° and 15° for fine impactors and between 12° and 36° for middle and coarse grains were found. Mean values of the ejection and impact angle, for all 100 trajectories, are shown in Figure 7. The values for grain sizes over 500 µm had to be handled with care, because there was only one trajectory recorded for each grain size. Therefore, significant information could only be made for smaller grain diameter. Figure 8 shows the mean ejection and impact angle for grain sizes between 140 and 280 µm.

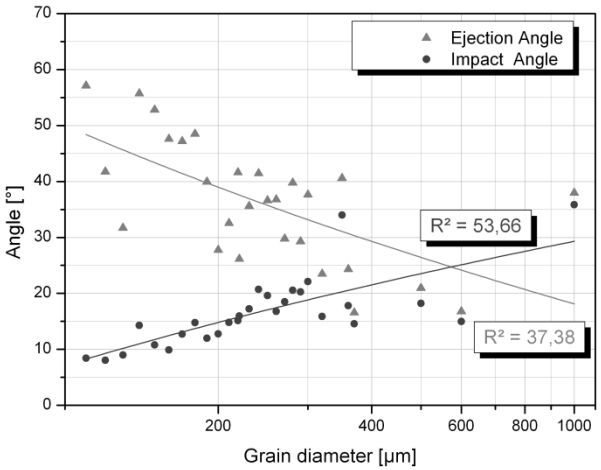

Figure 7: *Mean values of the ejection and impact angle, for all 100 trajectories. To both series, a logarithmic regression was fitted. A decreasing trend for the mean ejection angle (triangle) with increasing grain diameter is apparent in the plotted data. The mean impact angle (dots) increase with increasing grain diameter.*

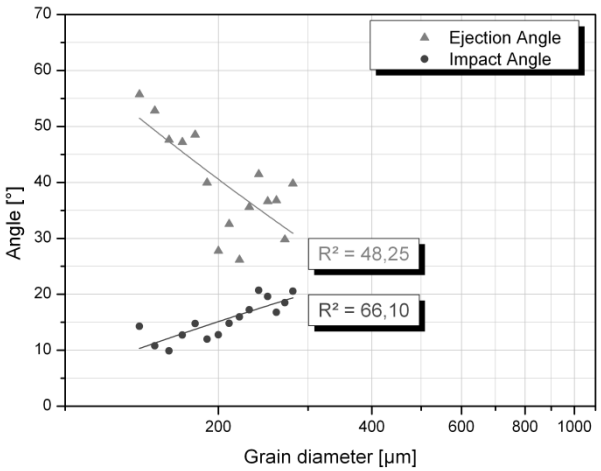

Figure 8: *Mean values of the ejection and impact angle for grain sizes from 140-280 µm. To both series, a logarithmic regression was fitted. The decreasing trend for the mean ejection angle (triangle) with increasing grain diameter is more significant than in Figure 7. Also for the mean impact angle, the increasing trend with increasing grain diameter is even better than in Figure 7.*

The mean ejection angle over all 100 evaluated trajectories was 41.7° and the mean impact angle was 15.15°. Additionally the ratio between the mean ejection angle α and mean impact angle β, which decrease with increasing grain diameter (Rice et al., 1995), could be confirmed. Figure 9 shows the ratio between the mean ejection angles and the mean impact angles of the 100 selected trajectories. The decreasing trend of the ratio is perceptible.

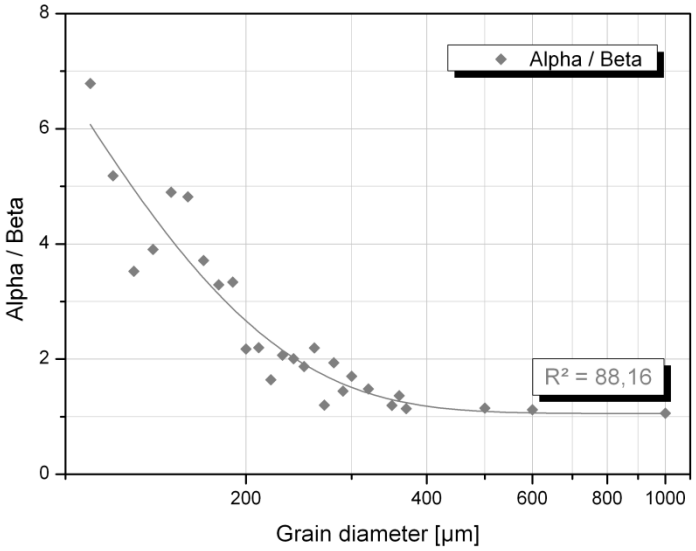

Figure 9: *The ratio between the mean ejection angle and the mean impact angle decreases with increasing grain diameter. An exponential regression was fitted to the serie.*

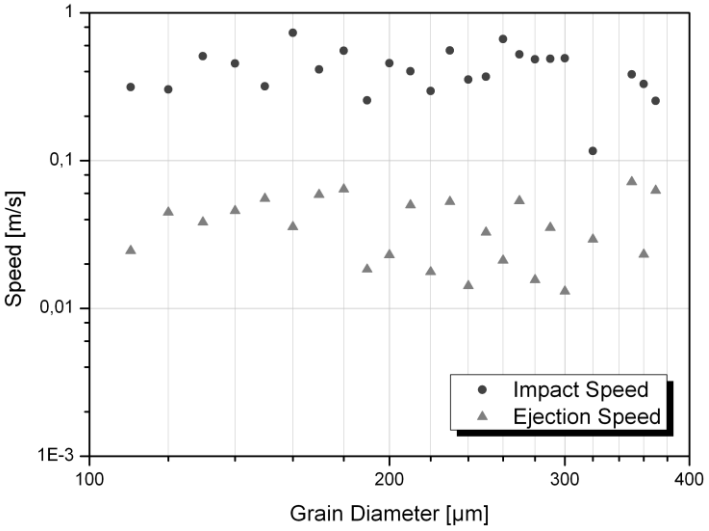

Figure 10: *Mean ejection and mean impact speed for grain sizes from 110-400 µm. The grains ejected from the bed had an average speed of one order of magnitude less than the impact speed.*

The results for ejection and impact speed of the saltating grains could be summarized as follows. Nalpanis et al. (1993) found values between 1.6 – 2.0 for the ratio u_i / u_e . Rice et al. (1995) confirmed also these results but they changed the ratio to u_e / u_i and got values of 0.5 – 0.6. These results could not be confirmed. The ration between the mean ejection speed u_e and the mean impact speed u_i was found nearly the same for all determined grain sizes. The grains ejected from the bed had an average speed of one order of magnitude less than the impact speed. Also Beladjine et al. (2007) found this coherence, whereby the mean ejection speed is one order of magnitude less than the mean impact speed. Figure 10 shows the mean ejection and mean impact speed for grain sizes from 110-400 µm. The shortage of data for bigger grain sizes leads to no significant results. Also values for saltation length and saltation height were only available for smaller grain sizes. Values of the mean saltation length and mean saltation height for bigger grain sizes (>400 µm) in Figure 11 were only shown for the sake of completeness. For grain sizes between 110 and 400 µm the mean saltation height is one order of magnitude less than the mean saltation length. Looking at the saltation height as a function of the saltation length, a linear coherence was found. This means that, if the grain has jumped far the higher it has been flown, see Figure 12 (left). The mean saltation length of the 100 evaluated grains was 1.99 cm. On the contrary the mean saltation height was 2.4 mm. In Figure 12 (right), a 3D trajectory from the evaluation could be seen.

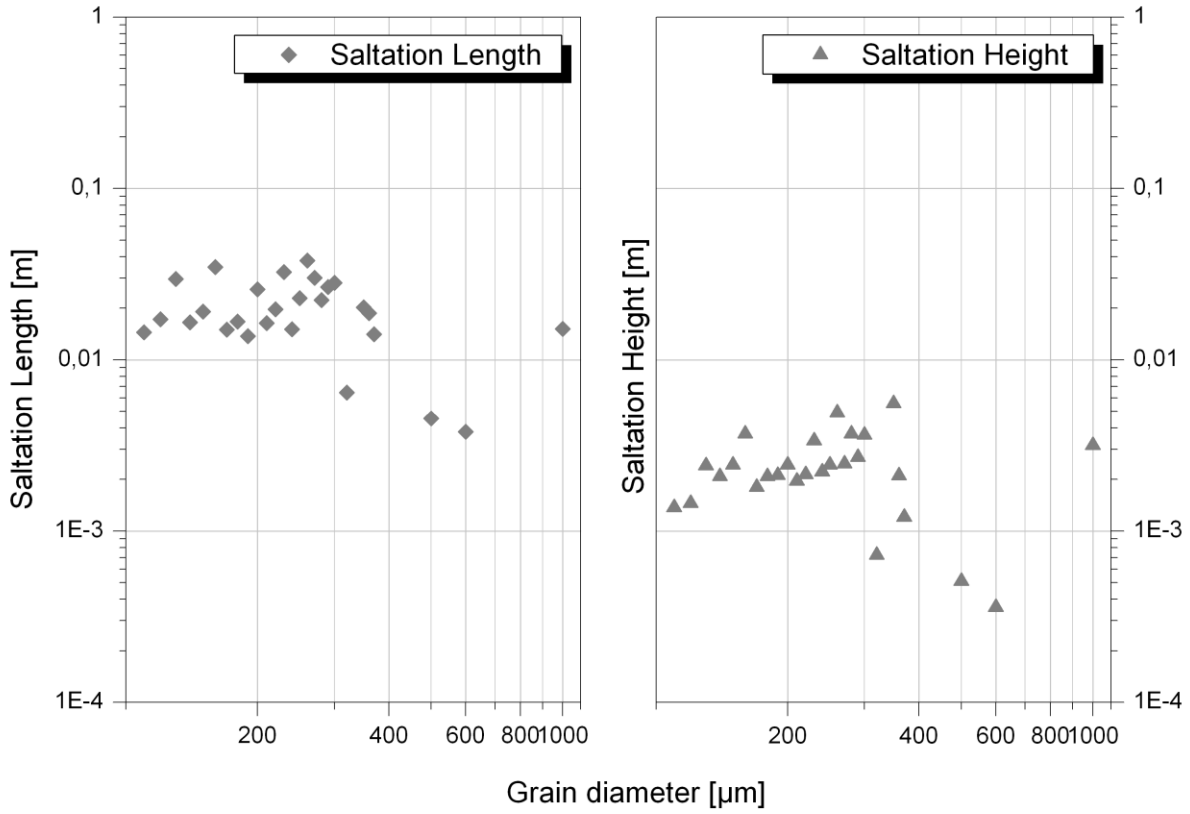

Figure 11: *Mean saltation length and mean saltation height for all 100 evaluated grains. For grain sizes between 110 and 400 µm the mean saltation height is one order of magnitude less than the mean saltation length.*

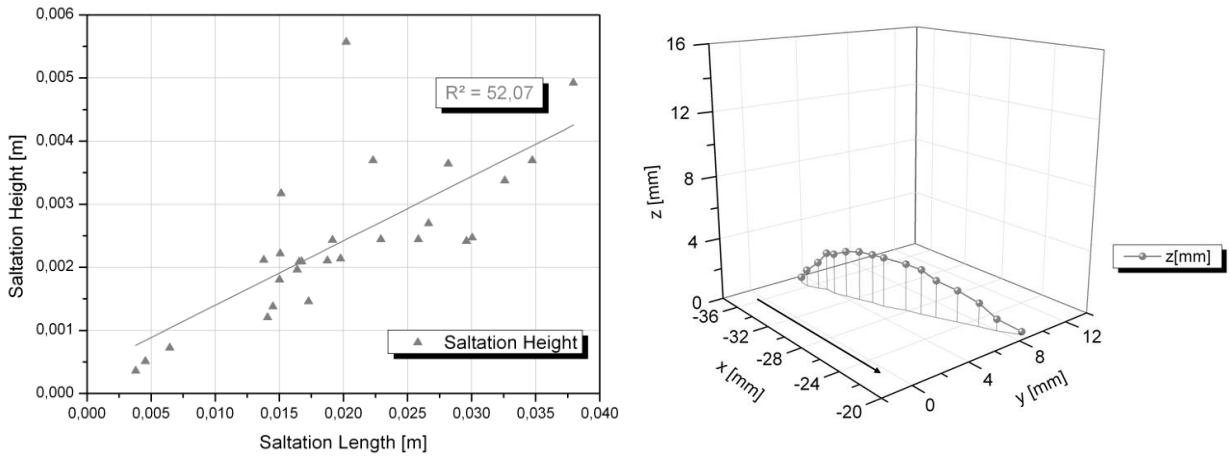

Figure 12: Left:*The saltation height as a function of the saltation length. A linear regression was fitted to the serie. The farer the grain has been jumped the higher it has been flown.* Right: *A 3D trajectory, of a saltating grain, measured at Zingst peninsula. The black arrowhead symbolizes the mean wind direction. The flange of the mirror is parallel to the x-Axis.*

5. CONCLUSION

With a new measurement setup, including a high-speed camera and a mirror plate, trajectories of saltating grains were characterized in 2D and 3D under natural and laboratory conditions. The trajectories were used to determine the ejection and impact angle, the ejection and impact speed as well as the saltation length and height of saltating grains. Also their size could have been calculated. The revealed results show, that high-speed film measurements in 3D are comparable to 2D measurements with high-speed photography presented in literature. The main striking results, obtained with the new system, can be summarized as follows.

- Ejection angles decrease with increasing grain diameter. They vary between 57° and 27° for fine and middle grains and between 38° and 20° for coarse grains. The mean ejection angle for all 100 evaluated trajectories was found with 41.7°.
- The impact angle increases with increasing grain diameter. Impact angles vary between 8° and 15° for fine grains and from 12 to 36° for middle and coarse grains. The mean impact angle for all 100 evaluated trajectories was found with 15.15°.
- Additionally the ratio between the mean ejection angle α and mean impact angle β, which decrease with increasing grain diameter (Rice et al., 1995), could be confirmed.
- The ration between the ejection speed u_e and impact speed u_i was found nearly the same for all determined grain sizes, but the grains ejected from the bed had an average speed of one order of magnitude less than the impact speed, which confirm the findings of Beladjine et al. (2007).
- The Runge-Kutta procedure is a good way to simulate the trajectory of the grain by using real measured values of the mean wind speed and fitting them to the measured trajectory of the saltating grain.
- With the calculated RMSE for each simulated grain diameter of a trajectory, picking the grain diameter with the lowest RMSE compared to the measured grain, it is possible to determine the diameter of the measured saltating grain.

The first measurements with the new camera system presented here, indicate the potential of 3D trajectory analysis. However, further effort has to put into the system to improve the estimation of the grain diameter and the calculation of the RMSE with reference to the trajectory.

REFERENCES

Anderson, R.S. and Haff, P.K. *Simulation of Eolian Saltation*. Science VOL. 241, Pages 820 - 823, 1988

Anderson, R.S. and Haff, P.K., Acta Mechanica Suppl. 1, 21, 1991

Bagnold, R.A. *The Physics of Blown Sand and Desert Dunes*, 253 pp. reprinted by Chapman and Hall Methuen, London, 1954

Beladjine, D., Ammi, M., Oger, L. and Valance, A. *Collision process between an incident bead and a three-dimensional granular packing*. The American Physical Society, Physical Review E 75, 061305, 2007

Greeley, R. and Iversen, J.D. *Wind as a geological process on Earth, Mars, Venus, and Titan*. Cambridge University Press, The Pitt Building, Trumpington Street, Cambridge CB2 1RP, 1985

Julien, P.Y. *Erosion and Sedimentation*. Cambrigde University Press, 1995

Laity, J. *Deserts and Desert Environments*. Wiley-Blackwell, November 2008

McEwan, I.K. and Willetts, B.B. Acta Mechanica Suppl. 1, 53, 1991

Mitha, S., Tran, M.Q., Werner, B.T. and Haff, P.K. *The grain-bed impact process in aeolian saltation*. Acta Mechanica, 63, 14, Pages 267 - 278, 1986

Pye, K. *Aeolian dust and dust deposits*. Academic Press Inc. London LTD., 24-28 Oval Road, London NW1 7DX, 1987

Rice, M.A., Willetts, B.B. and McEvan, I.K. *An experimental study of multiple grain-size ejecta produced by collisions of saltating grains with a flat bed*. International Association of Sedimentologists, Sedimentology 42, Pages 695 - 706, 1995

Schönfeldt, H.-J. *Quantitative Bestimmung des äolischen Sedimenttransports*. F.- M. Chmielewski, T. Foken, Beiträge zur Klima- und Meeresforschung, Seiten 249 - 258, Berlin und Bayreuth, 2003

Shao, Y. *Physics and Modelling of Wind Erosion*. Atmospheric and Oceanographic Sciences Library, Kluwer Academic Publishers, 2000

Willetts, B.B. and Rice, M.A. *Collision in aeolian saltation*. Acta Mechanica, 14, Pages 255 - 265, 1986